Check for updates

Influences of riverbed siltation on redox zonation during bank filtration: a case study of Liao River, Northeast China

Jiamei Wang, Yumeng Yan, Jing Bai and Xiaosi Su

ABSTRACT

The upper part of riverbed sediment is one of the key interfaces between surface water and groundwater, and biogeochemical process in this interface has a profound influence on the chemistry of infiltrated water. The lithology and permeability of bed sediment is mainly controlled by variation in river hydrodynamic conditions. However, there have been few studies of the effect of riverbed siltation on the hydrochemistry and redox reactions of infiltrated water due to the high variability in these processes and challenges associated with sampling. This study selected and examined a river channel near a site of riverbank filtration by drilling on the floating platform and conducting microelectrode testing and high-resolution sampling. The hydrodynamic and chemical characteristics of pore water in and lithologic characteristics of riverbed sediment, the siltation, and redox zone were examined and compared. Differences in hydrodynamic conditions changed the lithology of riverbed sediment, consequently affecting redox reactions during the process of river water infiltration. Variations in siltation changed the residence time of pore water and organic matter content, which ultimately resulted in differences in extension range and intensity of redox reactions. This study provides a valuable reference for understanding the effect of riverbed siltation on water quality of riverbank infiltration.

Key words | redox zonation, riverbed sediment, siltation, surface water–groundwater interaction

Jiamei Wang
Jing Bai
Xiaosi Su (corresponding author)
College of Construction Engineering,
Jilin University,
Changchun 130026,
China
and
Institute of Water Resources and Environment,
Jilin University,
Changchun 130021,
China
E-mail: *suxiaosi@163.com*

Yumeng Yan
Jilin Water Science Research Institute,
Changchun 130022,
China

HIGHLIGHTS

- Riverbed siltation was examined by waterway drilling techniques.
- High-resolution sampling identified redox zoning under siltation.
- Riverbed siltation changed redox zoning at the river water–sediment interface.

INTRODUCTION

Surface water infiltration is an important category of surface water–groundwater interaction, and in particular, river bank filtration (RBF) increases groundwater recharge. RBF is widely used around the world as a sustainable source of drinking water (Ray *et al.* 2002; Tufenkji *et al.* 2002), as this technology reduces environmental problems resulting from overexploitation of water resources and alleviates water supply crises in some areas (Ray *et al.* 2003; Hu *et al.* 2016). RBF not only changes the hydraulic connection between the river and groundwater, but also dilutes the concentrations of pollutants as a large proportion of dissolved and suspended contaminants are removed from water during the infiltration process. The redox environment of sediment is changed due to the infiltration of

This is an Open Access article distributed under the terms of the Creative Commons Attribution Licence (CC BY 4.0), which permits copying, adaptation and redistribution, provided the original work is properly cited (http://creativecommons.org/licenses/by/4.0/).

doi: 10.2166/nh.2020.107

Downloaded from http://iwaponline.com/hr/article-pdf/51/6/1478/792246/nh0511478.pdf
by guest

oxygen-carrying surface water, which is believed to promote redox reactions and the degradation and removal of pollutants (Romero-Esquivel *et al.* 2017; Guo *et al.* 2018). Developing appropriate management to realizing the full benefits of RBF requires an understanding of the evolution of hydrogeochemistry during riverbank infiltration (Henzler *et al.* 2016).

The riverbed sediment zone constitutes the uppermost zone during water infiltration, and this zone shows the greatest variations in physical, chemical, and biological gradients between river water and groundwater. These characteristics of the river sediment zone make it a key interface within surface water–groundwater interactions (Sophocleous 2002; McLachlan *et al.* 2017). The biogeochemistry of riverbed sediment plays a vital role in maintaining groundwater quality and ecological security (Tufenkji *et al.* 2002). During surface water infiltration, microbial fermentation, aerobic respiration, denitrification, iron–manganese reduction, sulfate reduction, and other reaction processes act to degrade bioavailable organic matter in riverbed sediment, resulting in sequential redox zonation (Yuan 2017). The permeability of sediment to water infiltration is influenced by physical, chemical, and biological factors, such as flow conditions, dissolved organic matter, and the activity of microorganisms (Brunke & Gonser 1997). Siltation not only reduces riverbed sediment permeability and recharge intensity, but also changes the hydrodynamic conditions of bank infiltration, drives changes to environmental conditions at the sediment–water interface, and affects the evolution of biogeochemical reactions during infiltration (Brunke & Gonser 1997; Cardenas 2008; Smith & Lerner 2008; Hu *et al.* 2014). For example, the infiltration rate affects oxygen consumption within a certain range, with a low infiltration rate resulting in high oxygen consumption and an anoxic state. In addition, variation in river flow may affect the structure and function of the riverbed microbial community, thereby potentially impacting biogeochemical processes and water quality. Certain extreme weather conditions, such as inundation, also affect water quality of RBF (Ascott *et al.* 2016), as a shortened infiltration travel time under heavy rainfall can result in reduced removal of pathogens, heavy metals, suspended matter, dissolved organic carbon, and organic micropollutants during infiltration (Derx *et al.* 2013; Pazouki *et al.* 2016). Infiltration water residence time and redox condition are two main parameters determining the performance of RBF (Henzler *et al.* 2016). While some recent studies have reported on the effects of river morphology on hyporheic water exchange and the permeability of riverbed sediment (Zhang *et al.* 2017; Cheng *et al.* 2019), there remains a lack of research on the effects of river morphology on hydrochemistry. Past studies considered riverbed sediment to be a homogeneous and stable interface, ignoring the influence of factors such as scouring and siltation on redox zonation during bank filtration.

The study area of the current study was a riverside well field in Shenyang, northeast China, in which groundwater quality is characterized to be of poor quality with high contents of iron and manganese. Previous studies have classified groundwater redox zones in different water flow paths during bank filtration by analyzing the spatial and temporal distribution of groundwater environmental indices and chemical components (Su *et al.* 2017). Dissolved organic carbon (DOC) and sedimentary organic carbon (SOC), as major electron donors, show high variability in sequential redox reactions under differences in microbial activities along the horizontal and vertical flow directions (Su *et al.* 2018; Yuan *et al.* 2020).

The Liao River is a highly seasonal river, with low flow periods characterized by siltation of the channel, whereas incoming water flow and sediment concentration increase greatly during the flood period, resulting in an increase in the sediment transport capacity of the channel, channel scouring, and over-bank siltation. Water flow gradually reduces subsequent to the flood, with a concurrent decrease in the ability of water to carry sediment, resulting in a return to channel siltation conditions. Previous studies have shown that rivers under the influence of upstream runoff and a downstream reservoir show obvious seasonal scouring and a decrease in the permeability of bed sediment, resulting in a variability in bed sediment depth of as much as 10 cm (Hu *et al.* 2007; Huang 2014). Porewater concentrations of Fe, Mn, and As far exceed drinking water standards, and changes in concentrations of these elements in porewater are related to the siltation and scouring of bed sediment. The objectives of the present study were to: (1) analyze the spatial structure characteristics of the riverbed sediment of the Liao River; (2) identify differences in infiltration

Downloaded from http://iwaponline.com/hr/article-pdf/51/6/1478/792246/nh0511478.pdf
by guest

permeability of sediment within a transverse segment of the river; and (3) analyze the spatial distribution of pore water chemical components and identify variation in redox zoning of scoured and silted riverbed sediment.

STUDY AREA AND METHODS

Study area

The study area of the present study is located 40 km north of Shenyang, northeastern China (Figure 1), and is situated on an alluvial plain in the middle and lower reaches of the Liao River. The study area has a river accumulational landform geomorphic type, comprising mainly low floodplain with a surface elevation varying between 42.0 and 52.0 m above sea level. The study area falls within a temperate sub-humid monsoon climate zone, with an annual average rainfall and potential evaporation of 635.5 and 1,594 mm, respectively. The study area falls between the Tieling and Ma Hushan hydrological stations 27 and 20 km upstream and downstream, respectively, and the study area river reach has a width of ~250 m. Hydrologic observations of the study area indicate that water level and river discharge show clear seasonal variations, with maximums occurring in August and September and the flood period extending from June to October (Figure 2).

Geophysical exploration conducted in a previous study (Su *et al.* 2017) showed strong heterogeneity in the riverbed sediment (Figure 3). The sediment within the study area within the range of 22 m of the south bank and 14 m of the north bank of Liao River shows homogeneous characteristics with obvious stratification and low permeability. In contrast, sediment located in the middle of the riverbed showed high lateral variability and high permeability (Su *et al.* 2017). Grain size of sediment in the study area showed large variation, with sediment types including clay, silt, and sand. The uppermost layer of sediment of the south bank of ~0.5 m depth comprised silt. Surface silt thickness gradually decreased from the south bank to the main channel, and the surface silt thickness of the riverbed at the main channel ranged between 0 and 0.1 m.

Groundwater in the study area is stored in unconsolidated phreatic Quaternary aquifers over impermeable Tertiary glutenite, with Liao River being the main source of groundwater recharge. The aquifer is overlaid with loam and clayey soil with a thickness of ~50.0 m consisting of fine sand, medium-coarse sand containing gravel, sand,

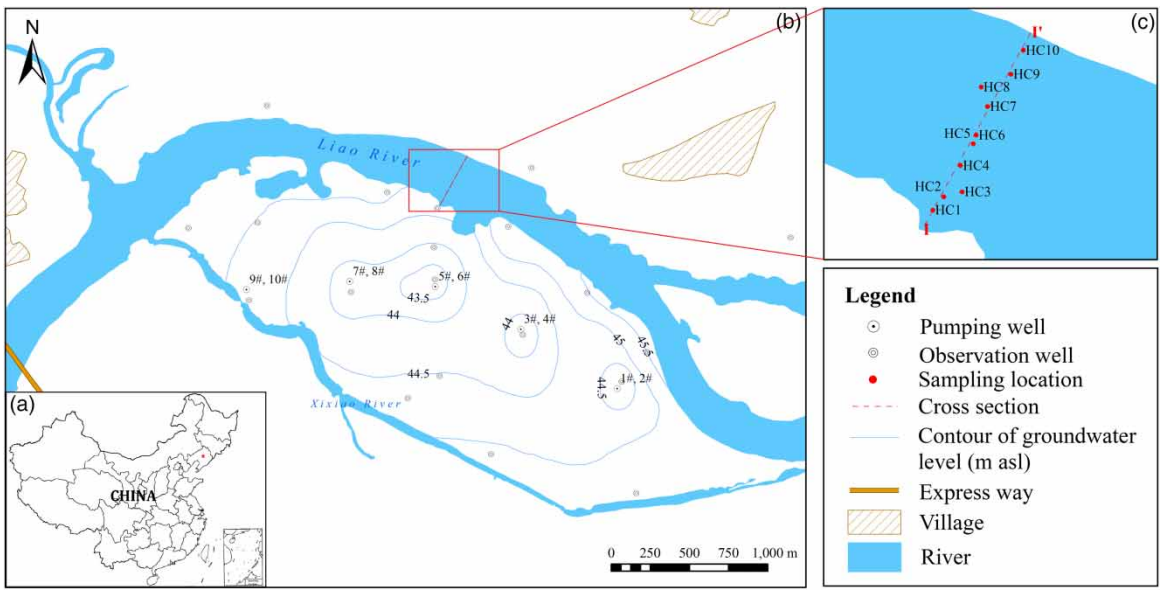

Figure 1 | (a) Inset map showing the location of the study area within China; (b) a higher resolution map showing the study reach and groundwater contours of the Liao river, Shenyang, northeastern China; (c) cross-section of the river showing sampling points.

Downloaded from http://iwaponline.com/hr/article-pdf/51/6/1478/792246/nh0511478.pdf
by guest

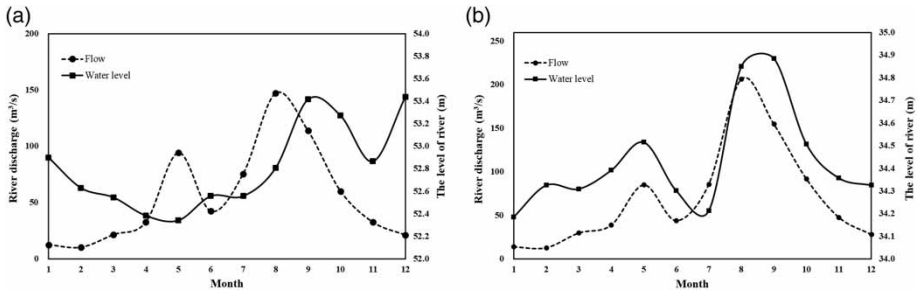

Figure 2 | Charts showing multi-year monthly average flow and water level within two sites along the Liao River, Shenyang, northeastern China (2015–2019): (a) Tieling hydrological station; (b) Ma Hushan hydrological station.

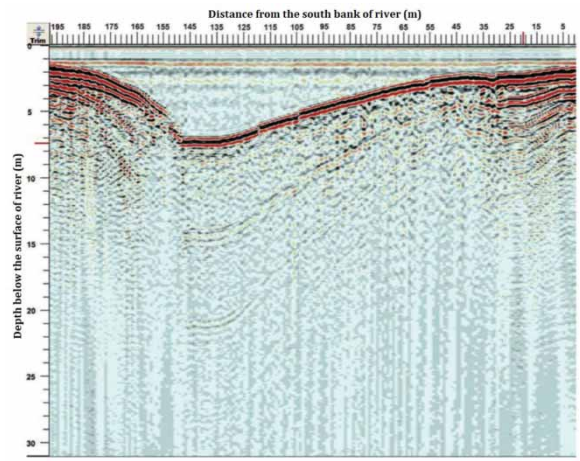

Figure 3 | Seismic wave geophysical profile of riverbed sediment of the Liao River, Shenyang, northeastern China (Su *et al.* 2017).

gravel and pebble, and coarse sand containing gravel. Ten pumping wells are distributed in the study area, with the cumulative yield of the pumps remaining stable for many years at ~30,000 $m^3\ d^{-1}$, resulting in several depression cones (Figure 1). The occurrence of two types of typical groundwater flow paths due to exploitation have been noted, namely shallow and deep flow paths. Groundwater flow along the shallow path through the silt layer flows at a slower rate of ~13.5 $m\ d^{-1}$ and has a long travel time. In contrast, the deep water flow path is characterized by good permeability and fast-flowing water, and has a closer hydraulic connection with river water (Su *et al.* 2017).

The chemistry of shallow groundwater of the study area is characterized as a Ca–Mg–HCO_3 or Ca–HCO_3 type, with iron and manganese concentrations of 2,809–4,261 mg kg^{-1} and 1,401–1,805 mg kg^{-1}, respectively. During bank infiltration, organic matter acts as the main electron donor, and the order of acceptors in terms of the degree of reactability is: O_2, NO_3^- > Mn (IV), and Fe (III) oxides or hydroxides > SO_4^{2-}. In fact, there is little difference in the horizontal extent of the redox zone between the shallow and deep flow paths, and the redox zone is controlled by the permeability of riverbed sediment and the aquifer at different depths (Su *et al.* 2018). The infiltration of river water from the Liao River into the groundwater acts as a vital water resource that is characterized by stable and good water quantity and quality.

Sampling and analysis

The riverbed section labeled 'I–I' (see Figure 1(c)) across the Liao River was selected as the control monitoring section in the present study as this section is consistent with the direction of the river infiltration and passes through the center of the groundwater drawdown funnel. Riverbed sediment and pore water samples were collected in September 2019 from the sampling locations shown in Figure 1(c).

For the collection of sediment samples, a mobile drilling platform was established over the Liao River and a portable high-frequency vibration drill (Wink S5 Vibracore, Canada) was used to collect sediment samples from a depth ≤5 m below the riverbed (see Table 1). The collected undisturbed sediment was packed in polyvinyl chloride (PVC) pipe, which was cut into 0.5 m segments. The segments were sealed with sample plugs and sealing film and then placed in an air-tight box for storage in refrigerator at a low temperature. The samples were transported to the laboratory as soon as possible for analysis and testing (Figure 4).

Downloaded from http://iwaponline.com/hr/article-pdf/51/6/1478/792246/nh0511478.pdf
by guest

Table 1 | Samples of riverbed sediment taken from the Liao River, Shenyang, northeastern China

Point	Distance to the south bank (m)	Sampling depth (m)
HC1	20	2.19
HC2	40	3.2
HC3	60	4.75
HC4	85	2.85
HC5	115	2.55
HC6	125	2.65
HC7	165	2.65
HC8	185	2.35
HC9	210	1.14
HC10	240	2.16

Sampling points are shown in Figure 1(c).

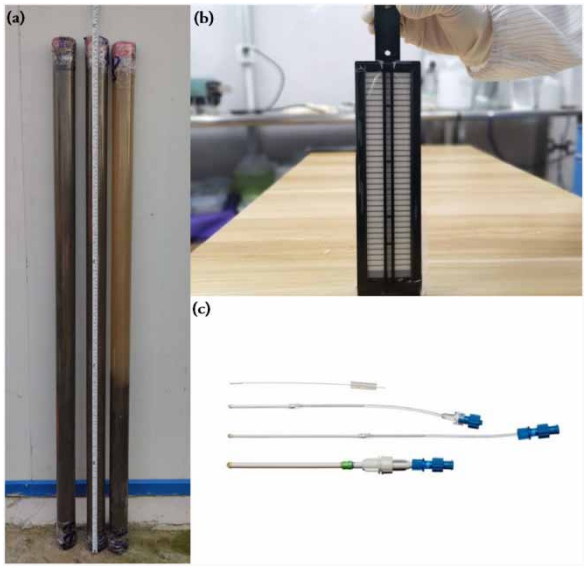

Figure 4 | Sampling device used for collection of sediment samples from the Liao River, Shenyang, northeastern China: (a) PVC pipes filled with sediment; (b) HR-Peeper sampler; (c) Rhizon samplers.

River water samples were collected in sampling tubes through siphoning, which ensured that the surface layer of the sediment remained undisturbed. The physico-chemical parameters of each sample were measured, after which the sample was transferred to a clean polyethylene bottle, sealed with a protective agent according to the test requirements, stored at low temperature (4 °C) and transported back to the laboratory for analysis and testing as soon as possible.

Pore water samples were collected from the upper 0–20 cm layer of sediment using an HR-Peeper sampler (High-resolution Peeper, Easy Sensor Ltd, China, Figure 4) (Xu *et al.* 2012). HR-Peepers were inserted into the sediment and retrieved after 48 h. Rhizon samplers (Rhizozphere Research Products, The Netherlands, Figure 4) were inserted into the sediment core through holes predrilled in the tube wall and pore water was collected from different depths below the 20 cm sediment layer using suction. During storage of pore water samples under refrigeration, the refrigerator was filled with nitrogen to avoid the influence of oxygen on subsequent tests.

Particle size distribution analysis was performed after sediment pretreatment through the use of screen analysis and a laser particle diameter analyzer (Bettersize2000, Dandong Better Instrument Co. Ltd, China). Microelectrodes (Unisense, Aarhus, Denmark) were used to measure oxidation–reduction potential (ORP), dissolved oxygen (DO), and pH of pore water samples. The accuracies of tests conducted were different at different sediment depths according to requirements, with precisions of 0.1 mm, 1, and 5 cm in the depth ranges of 0–1, 1–10, and 10–50 cm, respectively. Conventional anions (NO_3^-, SO_4^{2-}) in pore water were analyzed by ion chromatography (881-919 Compact IC, Metrohm, Herisau, Switzerland). Fe and Mn contents of pore water were measured by inductively coupled plasma mass spectrometry (ICP-MS, Agilent 7500 C, Agilent Technologies Inc., USA).

RESULT AND DISCUSSION

Structural and lithologic variation of riverbed sediment

Changes in river hydraulic conditions result in cycles of scouring and siltation, which affect the porosity, permeability, and lithology of the riverbed. The present study revealed the characteristics and variability of siltation by comparing hydrodynamic conditions at different points of the control section and relating these to the spatial distribution of lithology.

Hydrodynamic conditions

Hydrodynamic conditions of a river segment are driven by drops in the height of the river upstream and downstream,

Downloaded from http://iwaponline.com/hr/article-pdf/51/6/1478/792246/nh0511478.pdf
by guest

turbidity, and river channel morphology. A river flow rate that exceeds the threshold of bottom sediment critical transport velocity will result in the mobilization of bottom sediment and transport of this sediment downstream. The mobilization of bottom sediment will be enhanced during the rainy season due to higher river flows. This seasonal variation in hydrodynamic condition results in cycles of scouring and siltation of riverbed sediment, which in turn result in alternating changes in the permeability of the riverbed to water infiltration. Therefore, the river flow rate is an important index for quantifying hydrodynamic force. The river velocity and water depth at the monitored section were measured during September 2019 (Figure 5).

There were significant differences in hydrodynamic strength at the control section among the different sampling points along the cross-section, with the hydrodynamic strength of the north bank (concave bank) of the Liao River exceeding that of the south bank (convex bank), and the center of the riverbed showing the greatest hydrodynamic strength (HC7 point; river flow rate of 1.34 m s^{-1}). There was an obvious correlation between water depth and hydrodynamic condition, with the depth of water being positively related to the hydrodynamic intensity of the river. The riverbed section could be divided according to velocity and water depth into three zones of hydrodynamic intensity: (1) weak; (2) medium; and (3) strong (see Table 2).

Table 2 | Hydrodynamic zoning of the control section of the Liao River Shenyang, northeastern China

Hydrodynamic zoning	Flow rate (m s^{-1})	Water depth (m)	Points
Weak	0–0.4	0–2	HC1, HC2
Medium	0.4–1.2	2–4	HC3, HC4, HC5, HC6
Strong	>1.2	>4	HC7, HC8, HC9, HC10

Lithologic distribution of riverbed sediment

Riverbed sediment at different points showed stratification according to various characteristics, such as color and particle size (Figure 6). The lithology of the section could be described as mainly silty sand and fine sand, with silty soil and medium sand appearing at some points.

There were differences in the lithology of riverbed sediment among the different hydrodynamic zones, which was manifested as the thickness of the silt layer and average sediment particle size. The thickness of the silt layer was greater in the weak hydrodynamic zone compared with that in the medium hydrodynamic zone, while the silt layer in the strong hydrodynamic zone remained undeveloped. The rank of the zones according to the overall average particle size of sediment was: weak hydrodynamic zone < medium hydrodynamic zone < strong hydrodynamic zone. Therefore, there was a positive correlation between hydrodynamic condition and average particle size, which was consistent with the degree of riverbed scouring and clogging.

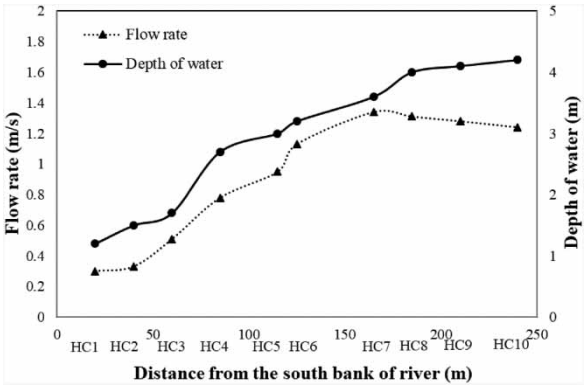

Figure 5 | Curves showing the river velocity and water depth at different sampling points along a cross-section of the control section of the Liao River, Shenyang, northeastern China. The locations of the sampling points along the cross section can be seen in Figure 1(c).

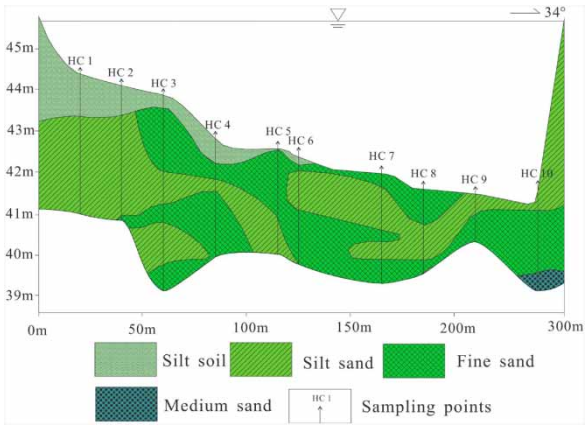

Figure 6 | The lithologic profile of riverbed sediment of the control section of the Liao River, Shenyang, northeastern China.

Downloaded from http://iwaponline.com/hr/article-pdf/51/6/1478/792246/nh0511478.pdf
by guest

The lithologic profile of riverbed sediment (Figure 6) indicated that the thickness of the silt layer can act as an indirect indicator of the degree of siltation and can therefore serve as an indicator of the siltation category of riverbed sediment. Since sedimentation had a considerable influence on hydrodynamic conditions up to a sediment depth of 50 cm, the control section was divided into three zones of siltation degree: (1) strong; (2) medium; and (3) weak. Subsequent analyses will be discussed in terms of siltation zone.

The silt layer developed on the surface layer of the riverbed at the strong siltation zone (HC1 and HC2). After prolonged siltation, a relatively thick and stable fine particle layer was formed, with a surface silty soil thickness of 70 cm and an average particle size of 34.39 μm. The lithology of the sediment layer was mainly silty soil and silty sand. The average particle size in the medium siltation zone (HC3, HC4, HC5, HC6) was 103.75 μm, significantly larger than that of the sediment in the strong siltation zone. For example, the thickness of the silty soil layer at sampling point HC6 was 22 cm, which was not as thick as that at the strong siltation zone of 70 cm. Lithology below a depth of 22 cm was interbedded silty sand and fine sand. However, there was no silty soil layer on the surface of the weak siltation zone (HC7, HC8, HC9, HC10), and no particles with average particle size <16 μm were found, with the maximum average particle size being ~500 μm. Interbedding of silty sand and fine sand occurred on the surface layer of the riverbed at HC7, which was as a result of differences in river hydrodynamic conditions among different periods, resulting in differences in the degree of sediment deposition.

Redox zoning in the hyporheic zone

Riverbed surface lithology changes during siltation, resulting in changes to the permeability of the riverbed. These changes in the riverbed permeability result in clear variations in the water infiltration rate, residence time, and redox zoning in riverbed sediment. The present study focused on examining riverbed sediment within a depth range ≤50 cm, as this sediment zone is the most affected by lithology and siltation. Variations in indices that are sensitive to redox reactions (NO_3^-, Mn^{2+}, Fe^{2+}, SO_4^{2-}) were analyzed based on environmental indicators (DO, ORP, pH) and pore water chemistry data. The present study then compared redox reactions among the different siltation zones to reveal the effects of scouring and sedimentation on redox reactions.

Environmental indices

The DO of overlying water was 5.0–5.5 mg L^{-1}, whereas that of pore water was reduced to <1 mg L^{-1} at a sediment depth of 5 mm. There were differences in the depths at which DO reached the detection limit among the different siltation conditions (Figure 7(a)), with the higher the degree of siltation, the shallower the depth at which DO reached the detection limit. Strong siltation resulted in an increased pore water travel time and a decrease in the depth at which DO decreased below the detection limit.

The ORP of overlying water was ~400 mV, indicating a relatively strong oxidation environment. The changes in ORP with depth were similar among different siltation zones (Figure 7(b)). Aerobic respiration occurred at a riverbed sediment depth ≤1 cm, and the decline in DO resulted in pore water moving from a relatively strong oxidizing environment to a weak oxidizing environment, with a rapid decrease in ORP. ORP fluctuated slightly within a depth range of 1–50 cm, whereas the redox environment remained basically stable.

The pH range of overlying water ranged between 7.5 and 8.5 with no obvious differences among the three siltation zones (Figure 7(c)). The pH of pore water remained basically stable between 7.0 and 8.0 with increasing sediment depth. There was a significant decrease in the pH of the surface layer of strong siltation zone. This observation can be explained by the longer residence time and sufficient biological respiration, which resulted in a greater production of CO_2 for release into the water and a consequent decrease in pH.

Redox reaction sensitivity indices

Monitoring of the redox sensitivity indices (O_2, NO_3^-, Fe^{2+}, Mn^{2+}, SO_4^{2-}, etc.) or the contents of reducing products (NH_4^+, HS^-, Fe^{2+}, CH_4, etc.) in pore water (Appelo & Postma 2004) can be used to identify redox zones during surface water infiltration. As shown in Figure 8, the present study constructed curves showing the changes in redox

Downloaded from http://iwaponline.com/hr/article-pdf/51/6/1478/792246/nh0511478.pdf
by guest

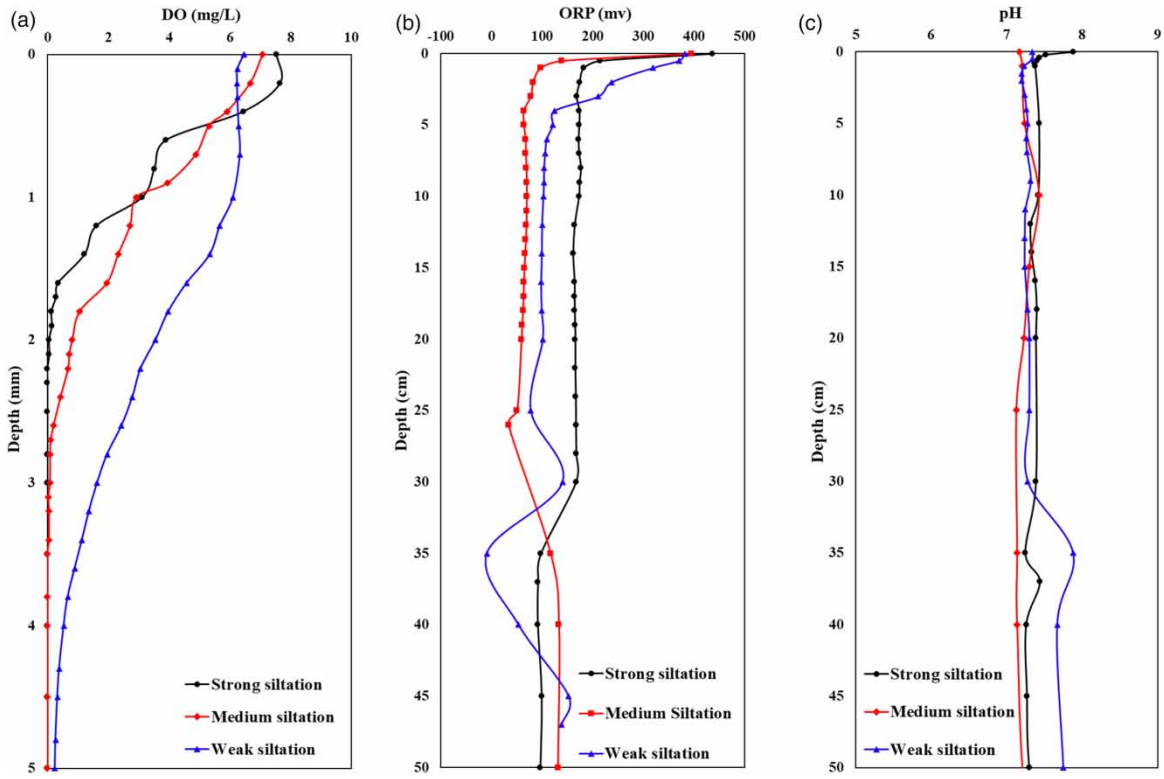

Figure 7 | The profiles of observed environmental indicators with changing riverbed sediment depth taken along a cross-section of the Liao River, Shenyang, northeastern China: (a) DO (DO < detection limit <5 mm depth is not shown), (b) ORP, and (c) pH value. The representative points of the strong, medium, and weak siltation zones were identified as HC2, HC6, and HC10, respectively.

products at different depths below the riverbed as an approach to identify the redox zones, with the results showing that the index changed regularly with the infiltration distance (Figure 8).

The overlying water of the control section showed a high concentration of NO_3^- which was unevenly distributed (Figure 8(a)). The spatial variation in NO_3^- in the Liao River is due to the influence of fish and other aquatic organisms, and NO_3^- accumulates in the surface layer of riverbed sediment. The concentration of NO_3^- in pore water decreased significantly at a depth of $\leq$10 cm, with the depth of the sediment zone in which the decrease occurred different among the different siltation zones. The depths of the zones in which NO_3^- in pore water decreased significantly, which could be regarded as the positive reaction zones of nitrate reduction, were 5, 4, and 7.5 cm within the strong, medium, and weak siltation zones, respectively.

The concentration of Mn^{2+} in the overlying water was generally low, ranging from 0.051 to 1.854 mg L^{-1}, with the highest concentrations found in the center of the riverbed (Figure 8(b)). The concentration of Mn^{2+} peaked at a certain depth at points near the south bank (HC1, HC2, HC5), which could be attributed to the reduction of manganese oxide or hydroxide. However, Mn^{2+} at points furthest from the south bank (HC6, HC7, HC10) remained basically unchanged with depth, with no reduction of Mn within 50 cm.

The concentration of Fe^{2+} in the overlying water was low overall, with the highest Fe^{2+} concentration at HC2 with a value of as much as 0.283 mg L^{-1} (Figure 8(c)). The concentrations of Fe^{2+} appeared the peak only at some points (HC1, HC2) at a depth of $\leq$50 cm. There was no significant change in Fe^{2+} content far from the south bank, with no clear reduction in Fe.

The concentrations of SO_4^{2-} in the overlying water ranged from 20.347 to 56.435 mg L^{-1}, and were different among the different zones (Figure 8(d)). The degree of variation in SO_4^{2-} with depth was greatly different among the

Downloaded from http://iwaponline.com/hr/article-pdf/51/6/1478/792246/nh0511478.pdf
by guest

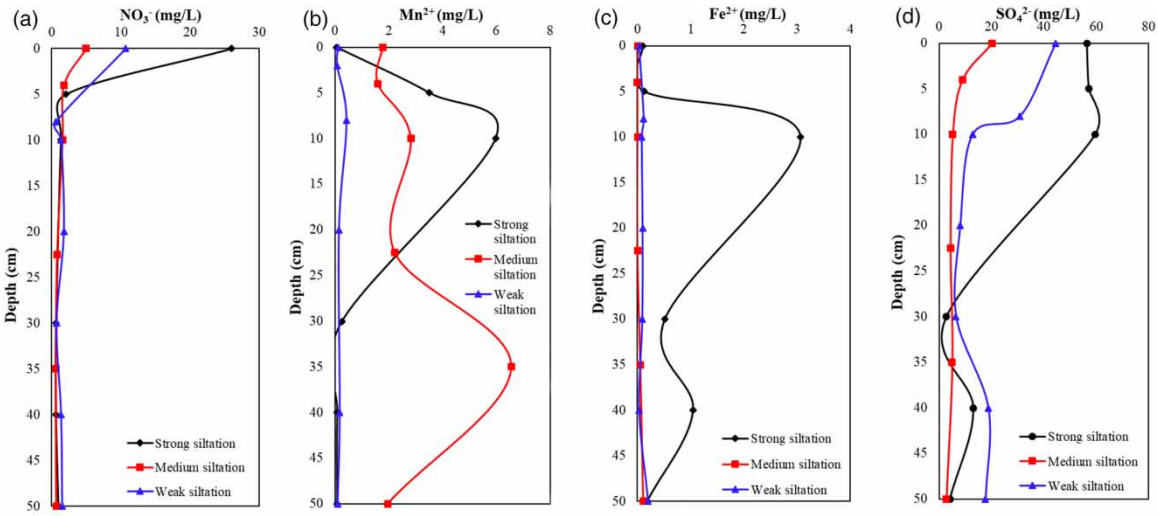

Figure 8 | Changes in the products of redox reactions with different depths of riverbed sediment taken along a cross-section of the Liao River Shenyang, northeastern China: (a) NO_3^-; (b) Mn^{2+}; (c) Fe^{2+}; (d) SO_4^{2-}.

different points. SO_4^{2-} concentrations showed clear increasing and decreasing trends at points close to the south bank (HC1, HC2). Therefore, sulfate reduction occurred at a depth $\leq$50 cm in the strong siltation zone, and sulfur oxidation also occurred at some points. SO_4^{2-} concentrations generally remained stable in the lower concentration range at points far from the south bank (HC5, HC6, HC7, HC10), and SO_4^{2-} reduction was relatively weak.

Redox zoning in riverbed sediment

Previous studies have been unable to identify a unified zoning standard and threshold for sequential redox zoning in the groundwater environment. The majority of past studies have determined the redox zonation threshold by the thermodynamic principle and the changes in concentration and the distribution characteristics of redox-sensitive indices in water (Lyngkilde *et al.* 1992).

Based on the analysis results of the environmental and hydrochemical indices of pore water, the present study determined that during the process of river water infiltration, oxidation–reduction occurs in the sediment–water interface under microbial action, with some ions participating as sequential electron acceptors. In addition, certain characteristics of redox zoning in the riverbed sediment were identified along the water flow path. The results showed that O_2 on the surface layer is the preferred electron acceptor during the initial stage of infiltration, and therefore, O_2 is the first electron acceptor to participate in the reaction. At the point at which oxygen is consumed up to a certain threshold, denitrification occurs, and there is a rapid decline in NO_3^- concentration. Since there will generally be overlaps between O_2 and NO_3^- in the reaction area, they will concurrently act as electron acceptors in an O_2/NO_3^- reduction zone. At a point at which the concentrations of O_2 and NO_3^- reduce to a lower value, reactions involving manganese and iron oxides or hydroxides in the riverbed sediment initiate, resulting in higher concentrations of Mn^{2+} and Fe^{2+}, i.e., the Mn (IV) reduction zone and the Fe (III) reduction zone. Since the reducibility of manganese exceeds that of iron, the Mn (IV) reduction zone will appear first. As infiltration continues, SO_4^{2-} will also participate in the redox reaction, forming an SO_4^{2-} reduction zone.

The present study determined the thresholds of redox zoning (Table 3) according to the characteristics of environmental and hydrochemical indices combined with the degree of siltation. The redox zoning during infiltration was categorized according to the changes in DO, NO_3^-, Fe^{2+}, Mn^{2+}, and SO_4^{2-} concentrations with riverbed sediment sampling depth (Figure 8), and each zone was named according to the most important redox reaction in a particular zone (Figure 9).

Downloaded from http://iwaponline.com/hr/article-pdf/51/6/1478/792246/nh0511478.pdf
by guest

Table 3 | Identification of indicators of redox zonation for a cross-section of the Liao River Shenyang, northeastern China

Redox zoning	DO	NO_3^-	Mn^{2+}	Fe^{2+}	SO_4^{2-}	ORP	pH
O_2/NO_3^-	≥LOD	Declining	Stable	Stable	Stable	Declining	Declining
Mn (IV))$^-$	<LOD	Stable	Peak	Stable	Stable	Stable	Stable
Fe (III)$^-$	<LOD	Stable	Stable	Peak	Stable	Stable	Stable
SO_4^{2-}	<LOD	Stable	Stable	Stable	Declining	Stable	Stable

LOD, limit of detection; DO, dissolved oxygen; ORP, oxidation–reduction potential.

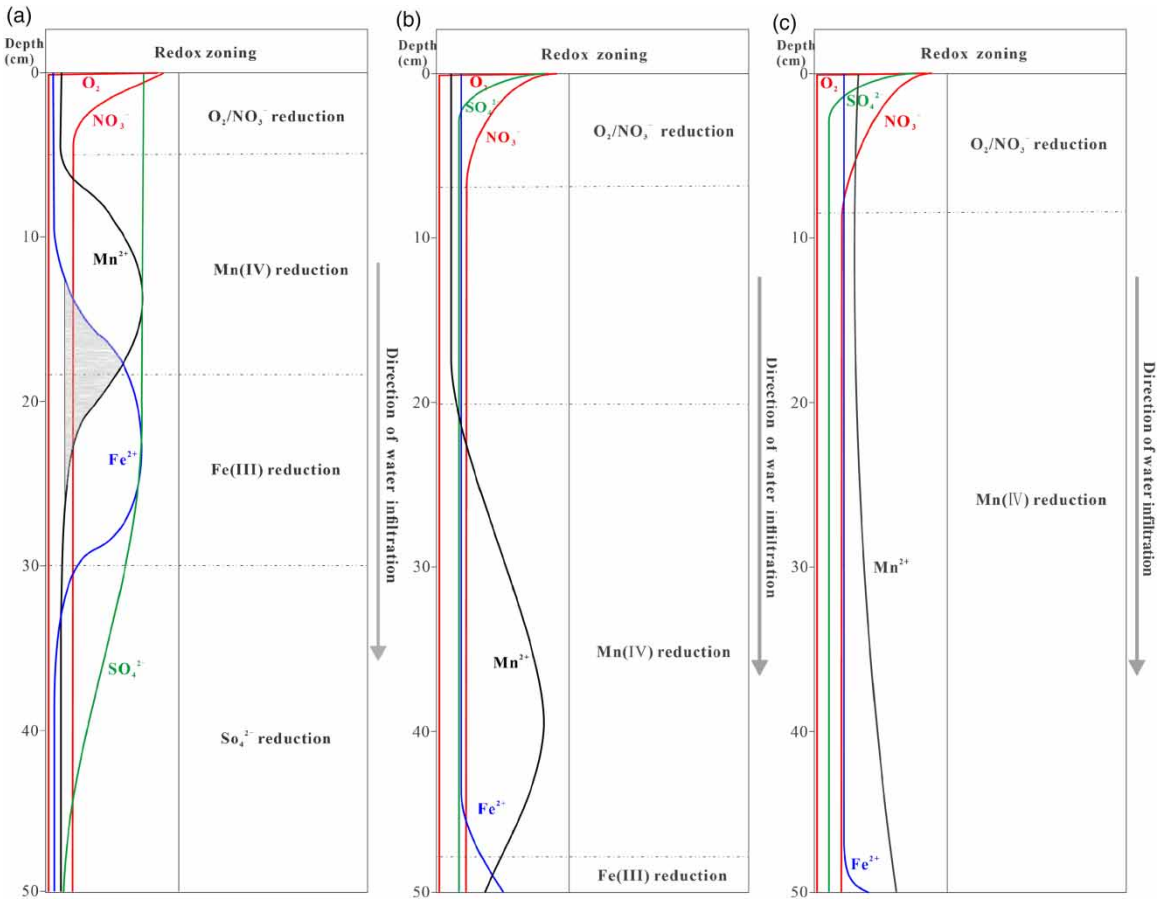

Figure 9 | Diagram showing the classification of redox zones for different siltation zones for a cross section of the Liao River, Shenyang, northeastern China: (a) strong siltation zone; (b) medium siltation zone; (c) weak siltation zone.

Within the strong siltation zone, O_2/NO_3^- reduction, Mn (IV) reduction, Fe (III) reduction, and SO_4^{2-} reduction were identified from the surface of the riverbed to a depth of 50 cm. Redox zoning was relatively dense, with some overlapping of zone points and a variety of simultaneous reduction reactions (Figure 9(a)). The strong siltation zone was characterized by fine lithology of the surface sediment, slow infiltration velocity, long residence time, and abundant organic matter, which provided enough electron donors to result in complex and abundant redox reactions.

Within the medium siltation zone, O_2/NO_3^- reduction and Mn (IV) reduction occurred in the riverbed sediment up to a depth of 50 cm, and there was a trend of Fe (III) reduction. However, no SO_4^{2-} reduction zone was evident

Downloaded from http://iwaponline.com/hr/article-pdf/51/6/1478/792246/nh0511478.pdf
by guest

(Figure 9(b)). Compared with the strong siltation zone, the silt layer of the medium siltation zone was thinner, the water infiltration rate was faster and the travel time was shorter in the middle part of the siltation zone, resulting in a decrease in organic matter content, which limited the degree of strength of redox reactions.

Within the weak siltation zone, only the O_2/NO_3^- reduction and Mn (IV) reduction zones appeared within the riverbed sediment depth up to 50 cm (Figure 9(c)). In contrast with the medium siltation zone, there was no complete Mn-reduction zone, indicating the presence of a large range of Mn (IV) reduction below 50 cm depth. Almost no silty soil was found on the surface layer, the overall lithology was coarse, water travel time was shorter, and there was a lower organic matter content, resulting in weaker redox reactions.

As shown in Table 4, the redox zonal ranges were identified by comparing and analyzing the redox sensitivity indices for different siltation zones. The degree of siltation was generally negatively correlated with the extension distance of the redox zoning in the riverbed sediment and positively correlated with the completeness of redox zoning. Due to the complex changes in hydrodynamic conditions, there were differences in mineral composition, and the action of microorganisms resulted in overlaps of the redox zones.

CONCLUSION

The present study analyzed the chemical composition and environmental indicators of pore water in riverbed sediment at different points along a cross-section of the Liao River, Shenyang, northeastern China. The observations of environmental and hydrochemical compositions of pore water were discussed in relation to differences in the degree of siltation. The riverbed sediment of the Liao River in the study area was divided into zones of strong, medium, and weak siltation under the influence of river hydrodynamics according to the different impacts on sediment permeability to water infiltration. Redox vertical zones within a riverbed depth of 50 cm were derived based on the three identified siltation zones from top to bottom into the zones of: (1) O_2/NO_3^- reduction; (2) Mn (IV) reduction; (3) Fe (III) reduction; and (4) SO_4^{2-} reduction. The strong siltation zone appeared to show overlapping redox zones, whereas Fe (III) reduction and SO_4^{2-} reduction appeared not to occur at the medium and weak siltation zones. The differences in the degree of siltation resulted in variation in infiltration time and organic matter content in sediment, and consequently in variation in the extension distance of redox zoning. The lithology of sediment and redox zoning during bank filtration were clearly impacted by scouring and siltation. However, the influence of scouring and siltation on organic matter and microorganisms requires further study. RBF management should pay attention to variations in riverbed sediment and redox zoning to avoid pollution of groundwater by river water and to realize the full benefits of bank filtration.

Table 4 | Ranges of redox zones in different siltation zones within a riverbed sediment depth of 50 cm for a cross-section of the Liao River Shenyang, northeastern China

	Depth (cm)			
Siltation zoning	**O_2/NO_3^- reduction**	**Mn (IV) reduction**	**Fe (III) reduction**	**SO_4^{2-} reduction**
Strong	0–5	5–25	8–30	10–50
Medium	0–7.5	7.5–50	–	–
Weak	0–8	8–50	–	–

'–' indicates unstudied.

ACKNOWLEDGEMENTS

The authors thank the editors of *Hydrology Research* and the reviewers for their thoughtful and constructive comments, which improved the manuscript.

FUNDING

This work was supported by the National Natural Science Foundation of China (grant nos: 41877178,41372238).

DATA AVAILABILITY STATEMENT

All relevant data are included in the paper or its Supplementary Information.

Downloaded from http://iwaponline.com/hr/article-pdf/51/6/1478/792246/nh0511478.pdf
by guest

REFERENCES

Appelo, C. A. J. & Postma, D. 2004 *Geochemistry, Groundwater and Pollution*, 2nd edn. A.A. Balkema, Leiden.

Ascott, M. J., Lapworth, D. J., Gooddy, D. C., Sage, R. C. & Karapanos, I. 2016 Impacts of extreme flooding on riverbank filtration water quality. *Science of the Total Environment* **554–555**, 89–101.

Brunke, M. & Gonser, T. O. M. 1997 The ecological significance of exchange processes between rivers and groundwater. *Freshwater Biology* **37** (1), 1–33.

Cardenas, M. B. 2008 Surface water-groundwater interface geomorphology leads to scaling of residence times. *Geophysical Research Letters* **35** (8), 307–315.

Cheng, D., Song, J., Wang, W. & Zhang, G. 2019 Influences of riverbed morphology on patterns and magnitudes of hyporheic water exchange within a natural river confluence. *Journal of Hydrology* **574**, 75–84.

Derx, J., Blaschke, A. P., Farnleitner, A. H., Pang, L., Blöschl, G. & Schijven, J. F. 2013 Effects of fluctuations in river water level on virus removal by bank filtration and aquifer passage – a scenario analysis. *Journal of Contaminant Hydrology* **147**, 34–44.

Guo, X., Zuo, R., Meng, L., Wang, J., Teng, Y., Liu, X. & Chen, M. 2018 Seasonal and spatial variability of anthropogenic and natural factors influencing groundwater quality based on source apportionment. *International Journal of Environmental Research and Public Health* **15** (2), 279.

Henzler, A. F., Greskowiak, J. & Massmann, G. 2016 Seasonality of temperatures and redox zonations during bank filtration – a modeling approach. *Journal of Hydrology* **535**, 282–292.

Hu, C., Wang, Y. & Shi, H. 2007 Evolution of trunk stream channel of Liaohe River and the runoff for sediment transport to maintain the stability of the river channel (In Chinese). *Journal of Hydraulic Engineering* **2**, 176–181.

Hu, H., Binley, A., Heppell, C. M., Lansdown, K. & Mao, X. 2014 Impact of microforms on nitrate transport at the groundwater–surface water interface in gaining streams. *Advances in Water Resources* **73**, 185–197.

Hu, B., Teng, Y., Zhai, Y., Zuo, R., Li, J. & Chen, H. 2016 Riverbank filtration in China: a review and perspective. *Journal of Hydrology* **541**, 914–927.

Huang, W. 2014 Analysis of riverbed change and evolution characteristics in Shifosi section of Liao River (In Chinese). *Water Resources & Hydropower of Northeast China* **09**, 23–24.

Lyngkilde, J., Christensen, T. H. & Christensen, T. H. 1992 Redox zones of a landfill leachate pollution plume (Vejen, Denmark). *Journal of Contaminant Hydrology* **10** (4), 273–289.

McLachlan, P. J., Chambers, J. E., Uhlemann, S. S. & Binley, A. 2017 Geophysical characterisation of the groundwater–surface water interface. *Advances in Water Resources* **109**, 302–319.

Pazouki, P., Prévost, M., McQuaid, N., Barbeau, B., De Boutray, M.-L., Zamyadi, A. & Dorner, S. 2016 Breakthrough of cyanobacteria in bank filtration. *Water Research* **102**, 170–179.

Ray, C., Grischek, T., Schubert, J., Wang, J. Z. & Speth, T. F. 2002 A perspective of riverbank filtration. *Journal American Water Works Association* **94** (4), 149.

Ray, C., Melin, G., Linsky, R. B. & SpringerLink 2003 *Riverbank Filtration. Improving Source-Water Quality*. Kluwer Academic Publishers, Secaucus.

Romero-Esquivel, L. G., Grischek, T., Pizzolatti, B. S., Mondardo, R. I. & Sens, M. L. 2017 Bank filtration in a coastal lake in South Brazil: water quality, natural organic matter (NOM) and redox conditions study. *Clean Technologies and Environmental Policy* **19** (8), 2007–2020.

Smith, J. W. N. & Lerner, D. N. 2008 Geomorphologic control on pollutant retardation at the groundwater-surface water interface. *Hydrological Processes* **22** (24), 4679–4694.

Sophocleous, M. 2002 Interactions between groundwater and surface water: the state of the science. *Hydrogeology Journal* **10** (1), 52–67.

Su, X., Lu, S., Lu, S., Gao, R., Su, D., Yuan, W., Dai, Z. & Papavasilopoulos, E. N. 2017 Groundwater flow path determination during riverbank filtration affected by groundwater exploitation: a case study of Liao River, Northeast China. *Hydrological Sciences Journal* **62** (14), 2331–2347.

Su, X., Lu, S., Yuan, W., Woo, N. C., Dai, Z., Dong, W., Du, S. & Zhang, X. 2018 Redox zonation for different groundwater flow paths during bank filtration: a case study at Liao River, Shenyang, northeastern China. *Hydrogeology Journal* **26** (5), 1573–1589.

Tufenkji, N., Ryan, J. N. & Elimelech, M. 2002 The promise of bank filtration. *Environmental Science & Technology* **36** (21), 422A–428A.

Xu, D., Wu, W., Ding, S., Sun, Q. & Zhang, C. 2012 A high-resolution dialysis technique for rapid determination of dissolved reactive phosphate and ferrous iron in pore water of sediments. *Science of the Total Environment* **421–422**, 245–252.

Yuan, W. 2017 *Biogeochemical Process of Fe and Mn During River Bank Infiltration Affected by Groundwater Exploiting (in Chinese)*. *PhD Thesis*.

Yuan, W. Z., Su, X. S., Bai, J., Xu, W., Wang, H. & Su, D. 2020 Response of microbial community structure to the hydrochemical evolution during riverbank filtration: a case study in Shenyang, China. *Human and Ecological Risk Assessment* **26** (3), 807–821.

Zhang, G., Song, J., Wen, M., Zhang, J., Jiang, W., Wang, L., Kong, F. & Wang, Y. 2017 Effect of bank curvatures on hyporheic water exchange at meter scale. *Hydrology Research* **48** (2), 355–369.

First received 31 July 2020; accepted in revised form 23 September 2020. Available online 21 October 2020

Downloaded from http://iwaponline.com/hr/article-pdf/51/6/1478/792246/nh0511478.pdf
by guest